*Journal of Elasticity* **74:** 147–173, 2004.



# On Invertibility of Elastic Single-Layer Potential Operator

R. VODIČKA[1] and V. MANTIČ[2]
[1]*Department of Mathematics, Faculty of Civil Engineering, Technical University of Košice, Vysokoškolská 4, 042 00 Košice, Slovakia. E-mail: roman.vodicka@tuke.sk*
[2]*Group of Elasticity and Strength of Materials, School of Engineering, University of Seville, Camino de los Descubrimientos s/n, 41092 Seville, Spain. E-mail: mantic@esi.us.es*

Received 8 August 2003

**Abstract.** The question of unique solvability of the boundary integral equation of the first kind given by the single-layer potential operator is studied in the case of plane isotropic elasticity. First, a sufficient condition of the positivity, and hence invertibility, of this operator is presented. Then, considering a scale transformation of the domain boundary, the well known formula for scaling the Robin constant in potential theory is generalized to elasticity. Subsequently, an explicit equation for evaluation of critical scales for a given boundary, when the single-layer operator fails to be invertible, is deduced. It is proved that there are either two simple critical scales or one double critical scale for any domain boundary. Numerical results, obtained applying a symmetric Galerkin boundary element code, confirm the propositions of the theory developed for both single and multi-contour boundaries.

**Mathematics Subject Classifications (2000):** 31A10, 31A25, 74B05, 74S15.

**Key words:** plane elasticity, single-layer potential, boundary integral equation of the first kind, solution uniqueness, logarithmic capacity, (symmetric Galerkin) boundary element method, condition number, multiply connected domain.

**Abbreviations:** BVP – Boundary Value Problem; BIE – Boundary Integral Equation; BEM – Boundary Element Method; SGBEM – Symmetric Galerkin Boundary Element Method.

## 1. Introduction

The Boundary Element Method (BEM), in both direct and indirect forms, usually leads in the case of a Dirichlet Boundary Value Problem (BVP) to the numerical solution of a Boundary Integral Equation (BIE) of the first kind with a single-layer potential operator. In plane elasticity, the weakly singular integral kernel of this operator, defined by the fundamental solution of the Navier equation, includes the logarithmic function. As a consequence of this fact, it is known that this integral operator may have a nontrivial null-space, thus the corresponding BIE does not have a unique solution. For a particular form of a domain boundary, whether such a situation takes place or not depends on the boundary size, making the problem dependent on the unit of length applied in the plane. Such

boundary sizes are usually referred to as critical (also exceptional or degenerate) scales.

The above phenomenon represents a well known difficulty appearing in applications of BIE's to the solution of other plane elliptic BVP's (e.g., defined by Laplace or biharmonic equation) as well. In potential theory the critical scale for a boundary is characterized by the zero value of the Robin constant or equivalently by the unit value of the logarithmic capacity (called also transfinite diameter) of this boundary, see [23, 25, 30]. Some approaches for avoiding the non-invertibility of the BIE obtained from the harmonic single-layer potential operator were studied in [5–7]. The problem of critical scales associated to the biharmonic single-layer potential has recently been analysed in depth in [9, 10, 15].

With reference to plane isotropic elasticity, a mathematical proof of the existence of critical scales has been given by Constanda [11]. Analytical and numerical approaches have been applied to determine critical scales for simple circular, elliptic or annular domains in [4, 19–21] and for a more general domain in [24]. Several ways of removing the zero eigenvalues in the resulting linear system caused by the critical scale (different from a simple re-scaling the domain or a modification of the fundamental solution, which are common approaches in BEM) were numerically tested in [24] as well. Theoretically well-based approaches of removing the non-uniqueness from the solution of the single-layer potential BIE were proposed in [13, 22].

The first objective of the present paper is to study conditions for the existence of a unique solution of the single-layer potential BIE in the case of plane isotropic elasticity. This question is closely related to the positivity of the single-layer operator for a particular boundary. The theory presented is based on the general theoretical results developed by Costabel and Dauge [15] and applied for the single-layer biharmonic potential operator therein. Some well-known properties of the elastic potentials and solutions of the pertinent BIE's either on bounded or unbounded domains analysed in [3, 14, 22, 28] are also applied. The other objective of the paper is to deduce a general formula, which enable to predict the values of the critical scales for a given boundary. The formula obtained, which further develops a result in [11], represents a generalization to elasticity of the well-known formula for scaling the Robin constant in potential theory. Similar formula for the biharmonic single layer potential has been given in [15]. Finally, the values of critical scales, obtained using the Symmetric Galerkin BEM (SGBEM) [2] and the former formula, are studied for several examples of boundary shapes (rectangle, ellipse, two circular holes, etc.). Comparisons with an analytical solution provided by the complex variable theory of plane elasticity [27] and with numerical calculations of other authors [4, 21] are given.

## 2. Single-layer Potential Solution of the Dirichlet Problem

Let us consider an elastic body defined by an open and connected set, a domain, $\Omega \subset \mathbb{R}^2$ with a bounded Lipschitz boundary [25] $\partial\Omega = \Gamma$ (i.e. given locally as

graphs of Lipschitz functions in a finite number of appropriate Cartesian coordinate systems, and $\Omega$ being locally on one side of $\Gamma$). Note, that $\Gamma$ may include corners but not cracks and cusps.

The boundary may include several components originating holes in the domain $\Omega$, which is then multiply connected. Let us denote $\Omega_m$, $m = 1, \ldots, H$, the bounded domains that form the holes in $\Omega$, where $H$ is the number of holes, and $\Gamma_m = \partial\Omega_m$ their respective boundaries. Let $\overline{\Omega}_m = \Omega_m \cup \Gamma_m$. When $\overline{\Omega}_m$ are added to $\Omega$, a domain without holes $\Omega_0$, a simply connected domain, with the boundary $\Gamma_0$ is obtained. If $\Omega$ is not bounded, then $\Omega_0 = \mathbb{R}^2$ and $\Gamma_0 = \emptyset$. A summary of these statements in mathematical formulae using a 'plus–minus' notation follows:

$$\begin{aligned} &\Omega = \Omega_0 \setminus \bigcup_{m=1}^{H} \overline{\Omega}_m, \qquad \Gamma = \bigcup_{m=0}^{H} \Gamma_m, \\ &\Omega_m^+ = \Omega_m, \qquad \Omega_m^- = \mathbb{R}^2 \setminus \overline{\Omega}_m, \quad m = 0, \ldots, H. \end{aligned} \tag{1}$$

Let $\boldsymbol{n}_m^{\pm}$ denote the two unit normal vectors defined almost everywhere on the boundary $\Gamma_m$ pointing outward with respect to the domains $\Omega_m^{\pm}$, respectively. A general case of a bounded domain $\Omega$ (hatched region) is shown in Figure 1.

Consider a fixed cartesian coordinate system $x_i$ $(i = 1, 2)$. Let $\boldsymbol{u} = (u_1, u_2)$ be the displacement solution of the following Dirichlet problem for the Navier equation in the case of plane strain state:

$$c_{ijkl} u_{k,lj}(x) = 0, \qquad x \in \Omega, \tag{2a}$$

$$u_i(x) = g_i(x), \quad x \in \Gamma, \tag{2b}$$

where the fourth-order tensor of elastic stiffnesses $c_{ijkl}$ is positive definite [17]

$$c_{ijkl} = \lambda \delta_{ij} \delta_{kl} + G(\delta_{ik}\delta_{jl} + \delta_{il}\delta_{jk}), \quad G > 0,\ 2G + 3\lambda > 0, \tag{3}$$

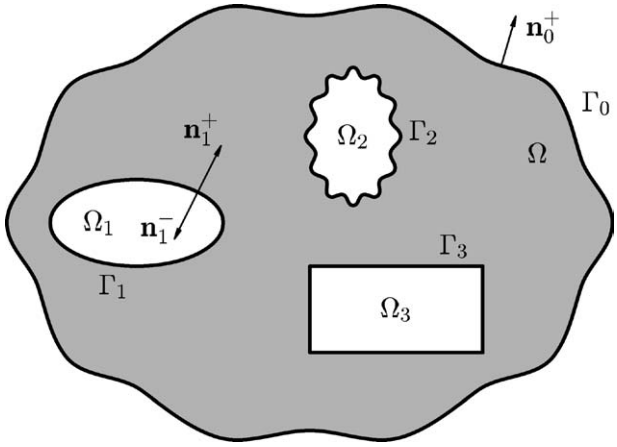


*Figure 1.* Description of a general bounded domain in 2D.

$\lambda$ and $G$ being Lamé constants and $\delta_{ij}$ being the Kronecker delta. Boundary tractions $\boldsymbol{t}$ associated to the outward pointing normal vector $\boldsymbol{n}$ at $\Gamma$ are obtained applying the traction operator $\boldsymbol{\mathcal{T}}_{\boldsymbol{n}}$ to displacements $\boldsymbol{u}$ as follows: $t_i = (\boldsymbol{\mathcal{T}}_{\boldsymbol{n}}\boldsymbol{u})_i = c_{ijkl}u_{k,l}n_j$.

Let $U_{ij}$, the symmetric second-order tensor of the fundamental solution of the Navier equation (2a), be given as:

$$U_{ij}(x, y) = \Lambda\left(-\kappa\delta_{ij}\ln|x-y| + \frac{(x_i - y_i)(x_j - y_j)}{|x-y|^2}\right), \tag{4}$$

where

$$\Lambda = \frac{1}{8\pi\, G(1-\nu)} > 0, \quad 7 > \kappa = 3 - 4\nu > 1, \tag{5}$$

$\nu$ being the Poisson ratio ($-1 < \nu < \frac{1}{2}$). Then, the solution $\boldsymbol{u}$ of (2) is expressed in the form of the single-layer potential

$$u_i(x) = \int_\Gamma U_{ij}(x, y)\varphi_j(y)\,\mathrm{d}\Gamma(y) = (\boldsymbol{U}\boldsymbol{\varphi})_i\,(x), \tag{6}$$

where the density $\boldsymbol{\varphi}$ represents a solution of the following BIE:

$$\boldsymbol{U}_\Gamma\boldsymbol{\varphi} = \boldsymbol{g}. \tag{7}$$

Here, the direct values of the single-layer potential $\boldsymbol{U}\boldsymbol{\varphi}(x)$ on the boundary $\Gamma$ are distinguished by the subscript $\Gamma$. Continuity of $\boldsymbol{U}\boldsymbol{\varphi}(x)$ across $\Gamma$ has been used in obtaining (7). Note that displacements $\boldsymbol{u} \in C^\infty(\mathbb{R}^2\setminus\Gamma)$ in (6) represent in fact a solution of Navier equation in $\mathbb{R}^2\setminus\Gamma$. Let $\boldsymbol{T}^*(x, y) = (\boldsymbol{\mathcal{T}}_{\boldsymbol{n}}\boldsymbol{U})(x, y)$ represent tractions associated to the fundamental solution at $x$. Then, considering asymptotic expansions of $\boldsymbol{U}(x, y)$ and $\boldsymbol{T}^*(x, y)$ for $|x| \to \infty$ and $y$ fixed, the following behaviour at infinity of $\boldsymbol{u}$ and the associated tractions $\boldsymbol{t}$ is obtained by direct verification [12, 23]:

$$\begin{aligned} u_i(x) &= U_{ij}(x, 0)b_j + \mathrm{O}(|x|^{-1}), \\ t_i(x) &= T^*_{ij}(x, 0)b_j + \mathrm{O}(|x|^{-2}), \end{aligned} \qquad b_j = \int_\Gamma \varphi_j(y)\,\mathrm{d}\Gamma(y), \quad |x| \to \infty. \tag{8}$$

Moreover, if $\Omega$ is an unbounded domain than $b_j = \int_\Gamma t_j(y)\,\mathrm{d}\Gamma(y)$.

Nevertheless, $\boldsymbol{U}_\Gamma$ in (7) is not always an invertible operator, or equivalently (7) has not always a (unique) solution. Thus, question of invertibility of $\boldsymbol{U}_\Gamma$ is crucial for solving (2) by means of (6). Some important properties of $\boldsymbol{U}_\Gamma$ concerning its invertibility are the subject of the theoretical analysis presented in the next section.

## 3. Properties of the Single-layer Potential Operator $\boldsymbol{U}_\Gamma$

The operator $\boldsymbol{U}_\Gamma$ is a continuous symmetric linear map between functional Sobolev spaces [14, 25, 28] of boundary tractions $[H^{-1/2}(\Gamma)]^2$ and boundary displacements

$[H^{1/2}(\Gamma)]^2$, i.e. $\boldsymbol{U}_\Gamma$: $[H^{-1/2}(\Gamma)]^2 \mapsto [H^{1/2}(\Gamma)]^2$. Note that $[H^{-1/2}(\Gamma)]^2$ is a dual space to $[H^{1/2}(\Gamma)]^2$. This duality extends an application of the inner product in the space of square Lebesgue-integrable functions $[L_2(\Gamma)]^2$ to functions $\hat{\boldsymbol{\varphi}} \in [H^{1/2}(\Gamma)]^2$ and $\boldsymbol{\varphi} \in [H^{-1/2}(\Gamma)]^2$, the integral $\int_\Gamma \hat{\varphi}_i \varphi_i \, \mathrm{d}\Gamma$ being considered in the generalized sense in what follows. Note that this integral represents, from the mechanical point of view, a kind of boundary energy. As follows from results in [14], $\boldsymbol{U}_\Gamma$ is strongly elliptic, which implies it is a Fredholm operator of index zero. Thus, its image $\boldsymbol{U}_\Gamma([H^{-1/2}(\Gamma)]^2)$ is a closed subspace, and the null-space dimension and the image codimension are finite and coincident.

Limits-to-the boundary of displacements and tractions defined outside of $\Gamma_m$ are considered here in the distributional (weak) sense by making use of the trace operators, which are well defined in classical sense for smooth functions in $\overline{\Omega}_m^{\pm}$ and whose values are extended to functions in the pertinent Sobolev spaces on $\Omega_m^{\pm}$ approximating these functions by smooth functions and applying the continuity of the trace operators (see [14, 25] for technical details).

### 3.1. POSITIVITY AND INVERTIBILITY

In Proposition 1 it is shown that $\boldsymbol{U}_\Gamma$ is positive on the subspace of tractions with zero resultant force on $\Gamma$. The next Remark 1 extends the scope of this proposition to contours more general than boundaries of (connected) domains. This fact will be required in the proof of the following Proposition 2, where it is shown that if the boundary $\Gamma$ is sufficiently small (meant in the applied unit of length, making the problem unit dependent), $\boldsymbol{U}_\Gamma$ is positive on the (complete) space of tractions and, subsequently, invertible on this space.

PROPOSITION 1. *Let $\Omega \subset \mathbb{R}^2$ be a domain with a bounded Lipschitz boundary $\Gamma$. If $\boldsymbol{\varphi} \in [H^{-1/2}(\Gamma)]^2$, $\boldsymbol{\varphi} \neq \mathbf{0}$, satisfies $\int_\Gamma \boldsymbol{\varphi} \mathrm{d}\Gamma = \mathbf{0}$, then $\int_\Gamma \varphi_i \left[\boldsymbol{U}_\Gamma \boldsymbol{\varphi}\right]_i \mathrm{d}\Gamma > 0$.*

*Proof.* Plane $\mathbb{R}^2$ is partitioned by $\Gamma$ in several connected open sets (domains), namely $\Omega$, $\Omega_m$ $(m = 1, \ldots, H)$ and $\Omega_0^-$. Note that $\Omega_0^- = \emptyset$ when $\Omega$ is unbounded. Let us denote $\boldsymbol{U}\boldsymbol{\varphi}(x) = \boldsymbol{u}_\varphi(x)$ for $x \in \mathbb{R}^2$. Then, $\boldsymbol{u}_\varphi$ is a solution of Navier equation in $\mathbb{R}^2 \setminus \Gamma$. Let traction vectors $\boldsymbol{t}_\varphi^{\pm}$ defined on $\Gamma_m$ and associated to the normal vector $\boldsymbol{n}_m^+$ represent the limits-to-the boundary of tractions defined in the neighbourhood of $\Gamma_m$ inside the domains $\Omega_m^{\pm}$ respectively. Let $m_0 = 0$ when $\Omega$ is bounded and $m_0 = 1$ when it is unbounded.

Consider first, that $\Omega$ is bounded. Then, the partial integration formula gives directly for bounded domains $\Omega$ and $\Omega_m^+$ $(m = 1, \ldots, H)$

$$\int_\Omega c_{ijkl} \frac{\partial u_{\varphi i}}{\partial x_j} \frac{\partial u_{\varphi k}}{\partial x_l} \, \mathrm{d}\Omega = \int_{\Gamma_0} t_{\varphi\ i}^+ u_{\varphi i} \mathrm{d}\Gamma - \sum_{m=1}^{H} \int_{\Gamma_m} t_{\varphi\ i}^- u_{\varphi i} \, \mathrm{d}\Gamma, \tag{9}$$

and

$$\int_{\Omega_m^+} c_{ijkl} \frac{\partial u_{\varphi i}}{\partial x_j} \frac{\partial u_{\varphi k}}{\partial x_l} \, \mathrm{d}\Omega = \int_{\Gamma_m} t_{\varphi\ i}^+ u_{\varphi i} \, \mathrm{d}\Gamma, \tag{10}$$

whereas this formula cannot be applied directly for the unbounded domain $\Omega_0^-$. Let $\Omega_R$ and $\Gamma_R$ respectively denote the circular disk and circumference of radius $R$ centered in the origin of coordinates, i.e. $\Omega_R = \{x \in \mathbb{R}^2 \mid |x| < R\}$. Then, taking a sufficiently large $R$, the partial integration formula applied to $\Omega_0^- \cap \Omega_R$ gives

$$\int_{\Omega_0^- \cap \Omega_R} c_{ijkl} \frac{\partial u_{\varphi i}}{\partial x_j} \frac{\partial u_{\varphi k}}{\partial x_l} \, \mathrm{d}\Omega = - \int_{\Gamma_0} t^-_{\varphi\, i} u_{\varphi i} \, \mathrm{d}\Gamma + \int_{\Gamma_R} t^+_{\varphi\, i} u_{\varphi i} \, \mathrm{d}\Gamma. \tag{11}$$

Letting $R \to \infty$, the last integral in (11) behaves, taking into account (8) and assumptions of this proposition, as $\mathrm{O}(R^{-2})$. Hence, in the limit $R \to \infty$ we obtain

$$\int_{\Omega_0^-} c_{ijkl} \frac{\partial u_{\varphi i}}{\partial x_j} \frac{\partial u_{\varphi k}}{\partial x_l} \, \mathrm{d}\Omega = - \int_{\Gamma_0} t^-_{\varphi\, i} u_{\varphi i} \, \mathrm{d}\Gamma. \tag{12}$$

Summing relations (9), (10) and (12) we have

$$\int_{\mathbb{R}^2 \setminus \Gamma} c_{ijkl} \frac{\partial u_{\varphi i}}{\partial x_j} \frac{\partial u_{\varphi k}}{\partial x_l} \, \mathrm{d}\Omega = \sum_{m=m_0}^{H} \int_{\Gamma_m} \left[ t^+_{\varphi\, i} - t^-_{\varphi\, i} \right] u_{\varphi i} \, \mathrm{d}\Gamma. \tag{13}$$

Relation (13) is also obtained for unbounded $\Omega$ by making use of the above procedure with the pertinent modifications: first, the partial integration formula is applied first to $\Omega \cap \Omega_R$ for a large $R$ and then the limit of the resulting relation is taken for $R \to \infty$, and second, the integral over $\Omega_0^-$ is not considered.

The right-hand side integral contains a product of the limit-to-the boundary of $\boldsymbol{u}_\varphi$, which is equal to $\boldsymbol{U}_\Gamma \boldsymbol{\varphi}$ due to the continuity of the single-layer potential across $\Gamma$, and the jump of the corresponding tractions across $\Gamma$, which due to the well-known jump relations for tractions of the single layer potential [3, 14] equals

$$\boldsymbol{t}^+_\varphi - \boldsymbol{t}^-_\varphi = \boldsymbol{\varphi}. \tag{14}$$

Hence, taking into account that $c_{ijkl}$ is a positive definite tensor [17], relation (13) writes as

$$0 \leqslant \int_{\mathbb{R}^2 \setminus \Gamma} c_{ijkl} \frac{\partial u_{\varphi i}}{\partial x_j} \frac{\partial u_{\varphi k}}{\partial x_l} \, \mathrm{d}\Omega = \int_\Gamma \varphi_i [\boldsymbol{U}_\Gamma \boldsymbol{\varphi}]_i \, \mathrm{d}\Gamma. \tag{15}$$

The first integral in (15) vanishes iff $\boldsymbol{u}_\varphi$, and equivalently $\boldsymbol{U}\boldsymbol{\varphi}$, represents a rigid body motion inside each connected subdomain of $\mathbb{R}^2 \setminus \Gamma$. Then, the tractions associated to these displacements, $\boldsymbol{\mathcal{T}}_{\boldsymbol{n}} \boldsymbol{U}\boldsymbol{\varphi}$, vanish in $\mathbb{R}^2 \setminus \Gamma$, and, due to (14), $\boldsymbol{\varphi} = 0$ on $\Gamma$. This completes the proof. □

REMARK. The former proposition is also valid for subsets of $\mathbb{R}^2$ with a more general topology. Let $\Theta \subset \mathbb{R}^2$ be a union of a finite number of non-intersecting bounded open and connected components (domains) $\Theta_m$, $m = 1, \ldots, C_\Theta$. Let its boundary $\partial\Theta = \Gamma$ be a union of a finite number of closed Lipschitz curves $\Gamma_m, m =$

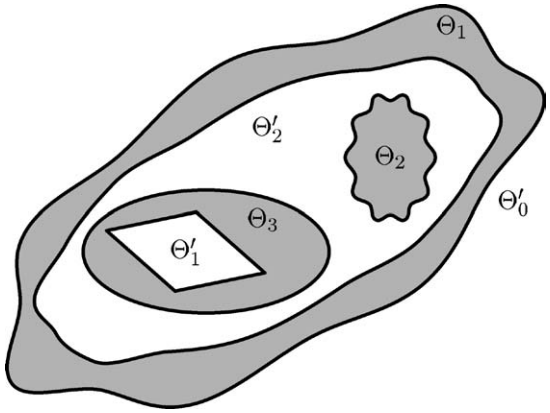


*Figure 2.* A case of $\Gamma$ which is not a boundary of any connected domain.

$1, \ldots, C_\Gamma$, which do not intersect each other. Let $\Theta' = \mathbb{R}^2 \setminus \overline{\Theta}$ be given by a union of non-intersecting open and connected components $\Theta'_m$, $m = 0, \ldots, C_{\Theta'}$, where only $\Theta'_0$ is unbounded and the others components are bounded. Note that equality $C_\Gamma = C_\Theta + C_{\Theta'}$ (called Alexander's relation) is valid [16]. Then Proposition 1 holds for $\Theta$ and $\Gamma$ as well.

For the sake of brevity the proof of this statement, based on the proof of Proposition 1, is only sketched here for a particular case of $\Theta$ depicted in Figure 2. Hence, we have $\Theta = \Theta_1 \cup \Theta_2 \cup \Theta_3$ (represented by hatched regions in the figure) and $\Theta' = \Theta'_0 \cup \Theta'_1 \cup \Theta'_2$, thus $C_\Theta = 3$ and $C_{\Theta'} = 2$. We have just to reconsider some relations of the previous proof. Relations analogous to (9)–(12) are valid for the following domains: (9) for $\Theta_1$, $\Theta_3$ and $\Theta'_2$, (10) for $\Theta_2$ and $\Theta'_1$, and (12) for $\Theta'_0$. Summing all these relations together we obtain a formula of the form (13), where $C_\Gamma$ appears instead of $H$, and $m_0 = 1$. A generalization of the example geometry and application of the same reasoning as used in the proof of the proposition renders (15) and, subsequently, also positiveness of $\boldsymbol{U}_\Gamma$ for any supposed $\Gamma$, given as a union of a finite number of not-intersecting closed Lipschitz curves, in the subspace of functions with vanishing integral over $\Gamma$.

Consider the following basis of the space of rigid body translations in plane:

$$\boldsymbol{\mu}^1(x) = \begin{Bmatrix} 1 \\ 0 \end{Bmatrix}, \qquad \boldsymbol{\mu}^2(x) = \begin{Bmatrix} 0 \\ 1 \end{Bmatrix}. \tag{16}$$

PROPOSITION 2. *Let $\Omega$ be a domain with a bounded Lipschitz boundary $\Gamma$. If $\Gamma$ is contained in the interior of a circular disk with radius $R = \mathrm{e}^{1/(2\kappa)}$, then $\boldsymbol{U}_\Gamma$ is positive (hence invertible) in $[H^{-1/2}(\Gamma)]^2$.*

*Proof.* Let $\Gamma_R$ denote the boundary of the disk with radius $R$ containing $\Gamma$. Proposition 1 together with Remark 1 imply that

$$\int_{\Gamma \cup \Gamma_R} \tilde{\varphi}_i [\boldsymbol{U}_{\Gamma \cup \Gamma_R} \tilde{\boldsymbol{\varphi}}]_i \, \mathrm{d}\Gamma > 0 \tag{17}$$

for nonzero $\tilde{\boldsymbol{\varphi}} \in [H^{-1/2}(\Gamma \cup \Gamma_R)]^2$ satisfying

$$\int_{\Gamma \cup \Gamma_R} \tilde{\varphi}_i \, \mathrm{d}\Gamma = 0. \tag{18}$$

Let us take $\tilde{\boldsymbol{\varphi}}$ in the form

$$\tilde{\boldsymbol{\varphi}} = \begin{cases} \boldsymbol{\varphi} & \text{on } \Gamma, \\ \displaystyle\sum_{k=1}^{2} \omega_k \boldsymbol{\mu}^k & \text{on } \Gamma_R, \end{cases} \tag{19}$$

with $\omega_k$ chosen so that (18) is satisfied. Let $c_i = \int_\Gamma \varphi_i \mathrm{d}\Gamma$. Condition (18) gives

$$0 = \int_{\Gamma \cup \Gamma_R} \tilde{\varphi}_i \, \mathrm{d}\Gamma = \int_\Gamma \varphi_i \, \mathrm{d}\Gamma + \int_{\Gamma_R} \sum_{k=1}^{2} \omega_k \mu_i^k \, \mathrm{d}\Gamma = c_i + 2\pi R \omega_i. \tag{20}$$

Decomposing the integral in (17) yields

$$\begin{aligned} 0 < & \int_\Gamma \varphi_i [\boldsymbol{U}_\Gamma \boldsymbol{\varphi}]_i \, \mathrm{d}\Gamma \\ & + \int_\Gamma \varphi_i(x) \left[ \int_{\Gamma_R} U_{ij}(x,y) \left( \sum_{k=1}^{2} \omega_k \mu_j^k(y) \right) \mathrm{d}\Gamma(y) \right] \mathrm{d}\Gamma(x) \\ & + \int_{\Gamma_R} \left( \sum_{k=1}^{2} \omega_k \mu_i^k(x) \right) \left[ \int_\Gamma U_{ij}(x,y) \varphi_j(y) \mathrm{d}\Gamma(y) \right] \mathrm{d}\Gamma(x) \\ & + \int_{\Gamma_R} \left( \sum_{k=1}^{2} \omega_k \mu_i^k \right) \left[ \boldsymbol{U}_{\Gamma_R} \left( \sum_{k=1}^{2} \omega_k \boldsymbol{\mu}^k \right) \right]_i \mathrm{d}\Gamma, \end{aligned} \tag{21}$$

where the second and the third integrals are equal to each other due to the self-adjoint character of $\boldsymbol{U}$. When relations (20) are substituted into (21), the second and fourth integrals become respectively, according to [20, 21],

$$-\frac{\Lambda}{2}(-2\kappa \ln R + 1)(c_1^2 + c_2^2), \tag{22a}$$

and

$$\frac{\Lambda}{2}(-2\kappa \ln R + 1)(c_1^2 + c_2^2). \tag{22b}$$

Hence, we see that (21) becomes

$$0 < \int_\Gamma \varphi_i [\boldsymbol{U}_\Gamma \boldsymbol{\varphi}]_i \mathrm{d}\Gamma - \frac{\Lambda}{2}(-2\kappa \ln R + 1)(c_1^2 + c_2^2). \tag{23}$$

The second member vanishes for $R = \mathrm{e}^{1/(2\kappa)}$, therefore the integral in (23) must be positive for any nonzero $\boldsymbol{\varphi}$. □

The proposition gives an alternative how to safe (7) from having multiple solutions or being unsolvable by making use of a suitable unit of length resulting in sufficiently small dimensions of $\Gamma$.

### 3.2. SCALING

The main purpose of this subsection is first to prove that for a given $\Gamma$ there exist either one or two critical scale factors $\rho_c > 0$ such that $\boldsymbol{U}_{\rho_c\Gamma}$ has a nontrivial null-space, where

$$\rho\Gamma = \big\{\rho x \in \mathbb{R}^2 \mid x \in \Gamma\big\}, \tag{24}$$

and second to deduce a formula which allow us to evaluate these critical scales.

Let us introduce, see [15], a dilation operator $\boldsymbol{M}_\rho$, which maps functions defined on $\Gamma$ to functions defined on $\rho\Gamma$, as follows:

$$\begin{aligned} &\boldsymbol{M}_\rho\colon \big[H^{-1/2}(\Gamma)\big]^2 \mapsto \big[H^{-1/2}(\rho\Gamma)\big]^2, \\ &(\boldsymbol{M}_\rho\boldsymbol{\varphi})(\tilde{y}) = \boldsymbol{\varphi}\left(\frac{\tilde{y}}{\rho}\right) = \tilde{\boldsymbol{\varphi}}(\tilde{y}), \quad \tilde{y} \in \rho\Gamma. \end{aligned} \tag{25}$$

We can now calculate for any $\tilde{\boldsymbol{\varphi}} \in [H^{-1/2}(\rho\Gamma)]^2$ and any $x \in \Gamma$ the single-layer potential

$$\begin{aligned} &[\boldsymbol{U}_{\rho\Gamma}\tilde{\boldsymbol{\varphi}}]_i(\rho x) \\ &\quad = [\boldsymbol{U}_{\rho\Gamma}\boldsymbol{M}_\rho\boldsymbol{\varphi}]_i(\rho x) \\ &\quad = \int_{\rho\Gamma} \Lambda\left(-\kappa\delta_{ij}\ln|\rho x - \tilde{y}| + \frac{(\rho x_i - \tilde{y}_i)(\rho x_j - \tilde{y}_j)}{|\rho x - \tilde{y}|^2}\right)(\boldsymbol{M}_\rho\boldsymbol{\varphi})_j(\tilde{y})\,\mathrm{d}(\rho\Gamma)(\tilde{y}) \\ &\quad = \int_{\Gamma} \Lambda\left(-\kappa\delta_{ij}\ln|\rho x - \rho y| + \frac{(\rho x_i - \rho y_i)(\rho x_j - \rho y_j)}{|\rho x - \rho y|^2}\right)\varphi_j(y)\rho\,\mathrm{d}\Gamma(y) \\ &\quad = \rho\bigg[\int_{\Gamma} \Lambda\left(-\kappa\delta_{ij}\ln|x - y| + \frac{(x_i - y_i)(x_j - y_j)}{|x - y|^2}\right)\varphi_j(y)\,\mathrm{d}\Gamma(y) \\ &\qquad\quad - \int_{\Gamma} \Lambda\kappa\ln\rho\,\varphi_i(y)\,\mathrm{d}\Gamma(y)\bigg] \\ &\quad = \rho\bigg[[\boldsymbol{U}_\Gamma\boldsymbol{\varphi}]_i(x) - \Lambda\kappa\ln\rho\int_{\Gamma}\varphi_i\,\mathrm{d}\Gamma\bigg]. \end{aligned} \tag{26}$$

Note that, following Propositions 1 and 2, rigid body translations $\boldsymbol{\mu}^k(\Gamma)$ ($k = 1, 2$) might define a subspace, where $\boldsymbol{U}_{\rho\Gamma}$ is negative for $\rho$ sufficiently large. Scaling behaviour of $\boldsymbol{U}_\Gamma$ shown in (26) will allow us to prove this hypothesis.

LEMMA 1. *Let $\Omega$ be a domain with a bounded Lipschitz boundary $\Gamma$. Then, there exists a constant $\rho_M$ such that for all $\rho > \rho_M$ and for any $\hat{\boldsymbol{\mu}} = \alpha_1\boldsymbol{\mu}^1 + \alpha_2\boldsymbol{\mu}^2 \neq \mathbf{0}$ $(\alpha_1, \alpha_2 \in \mathbb{R})$ it holds $\int_{\rho\Gamma}[\boldsymbol{M}_\rho\hat{\boldsymbol{\mu}}]_i[\boldsymbol{U}_{\rho\Gamma}\boldsymbol{M}_\rho\hat{\boldsymbol{\mu}}]_i \mathrm{d}(\rho\Gamma) < 0$.*

*Proof.* Recall that $\boldsymbol{\mu}^k(\rho x) = [\boldsymbol{M}_\rho\boldsymbol{\mu}^k](\rho x) = \boldsymbol{\mu}^k(x)$, $x \in \Gamma$, $k = 1, 2$. Then, we obtain, for any $\alpha_1, \alpha_2 \in \mathbb{R}$,

$$\begin{aligned}
&\int_{\rho\Gamma}\big[\boldsymbol{M}_\rho(\alpha_1\boldsymbol{\mu}^1 + \alpha_2\boldsymbol{\mu}^2)\big]_i\big[\boldsymbol{U}_{\rho\Gamma}\big(\boldsymbol{M}_\rho(\alpha_1\boldsymbol{\mu}^1 + \alpha_2\boldsymbol{\mu}^2)\big)\big]_i \mathrm{d}(\rho\Gamma)\\
&\quad= \rho^2\int_\Gamma(\alpha_1\mu_i^1 + \alpha_2\mu_i^2)\bigg(\big[\boldsymbol{U}_\Gamma(\alpha_1\boldsymbol{\mu}^1 + \alpha_2\boldsymbol{\mu}^2)\big]_i\\
&\qquad- \Lambda\kappa\ln\rho\int_\Gamma(\alpha_1\mu_i^1 + \alpha_2\mu_i^2)\mathrm{d}\Gamma\bigg)\mathrm{d}\Gamma\\
&\quad= \rho^2\bigg(\int_\Gamma(\alpha_1\mu_i^1 + \alpha_2\mu_i^2)\big[\boldsymbol{U}_\Gamma(\alpha_1\boldsymbol{\mu}^1 + \alpha_2\boldsymbol{\mu}^2)\big]_i\mathrm{d}\Gamma\\
&\qquad- \Lambda\kappa\ln\rho\bigg(\int_\Gamma(\alpha_1\mu_i^1 + \alpha_2\mu_i^2)\mathrm{d}\Gamma\bigg)^2\bigg)\\
&\quad= \rho^2\bigg(\int_\Gamma(\alpha_1\mu_i^1 + \alpha_2\mu_i^2)\big[\boldsymbol{U}_\Gamma(\alpha_1\boldsymbol{\mu}^1 + \alpha_2\boldsymbol{\mu}^2)\big]_i\,\mathrm{d}\Gamma\\
&\qquad- \Lambda\kappa\ln\rho(\alpha_1^2 + \alpha_2^2)\bigg(\int_\Gamma\mathrm{d}\Gamma\bigg)^2\bigg).
\end{aligned}\tag{27}$$

The last expression is obviously less than zero for sufficiently large $\rho$ and $\alpha_1^2 + \alpha_2^2 > 0$. □

Furthermore, Proposition 1 provides an excellent tool for using the results in [15, Section 3], the following lemma being satisfied by $\boldsymbol{U}_\Gamma$ (see also [3, Theorem 9.5.7]).

LEMMA 2 [15]. *Let $\boldsymbol{p}^k$ $(k = 1, 2)$ be a basis of a finite-dimensional subspace of $[H^{1/2}(\Gamma)]^2$ such that $\boldsymbol{U}_\Gamma$ is positive for all $\boldsymbol{\varphi} \in [H^{-1/2}(\Gamma)]^2$ satisfying $\int_\Gamma p_i^k\varphi_i\,\mathrm{d}\Gamma = 0$. Let the augmented operator $\widehat{\boldsymbol{U}}_\Gamma$ be defined as*

$$\begin{pmatrix}[H^{-1/2}(\Gamma)]^2\\ \times\\ \mathbb{R}^2\end{pmatrix} \ni \begin{pmatrix}\boldsymbol{\varphi}\\ \boldsymbol{\omega}\end{pmatrix} \overset{\widehat{U}_\Gamma}{\mapsto} \begin{pmatrix}\boldsymbol{U}_\Gamma\boldsymbol{\varphi} - \sum_{k=1}^2\omega_k\boldsymbol{p}^k\\ \\ \int_\Gamma p_i^k\varphi_i\,\mathrm{d}\Gamma\end{pmatrix} \in \begin{pmatrix}[H^{1/2}(\Gamma)]^2\\ \times\\ \mathbb{R}^2\end{pmatrix}.$$

*Then $\widehat{\boldsymbol{U}}_\Gamma$ is an isomorphism.*

Thus, due to Proposition 1, the system of equations

$$\boldsymbol{U}_\Gamma\boldsymbol{\varphi} - \sum_{k=1}^2\omega_k\boldsymbol{\mu}^k = \boldsymbol{g},\tag{28a}$$

$$\int_\Gamma \mu_i^k \varphi_i \, \mathrm{d}\Gamma = \int_\Gamma \varphi_k \, \mathrm{d}\Gamma = \xi_k, \quad k = 1, 2, \tag{28b}$$

has for each $\boldsymbol{g} \in [H^{1/2}(\Gamma)]^2$ and for each $\boldsymbol{\xi} \in \mathbb{R}^2$ a unique solution $\boldsymbol{\varphi} \in [H^{-1/2}(\Gamma)]^2$ and $\boldsymbol{\omega} \in \mathbb{R}^2$. Moreover, there exists a linear operator $\boldsymbol{B}_\Gamma\colon \mathbb{R}^2 \mapsto \mathbb{R}^2$, which for a given $\boldsymbol{\xi}$ and $\boldsymbol{g} = \boldsymbol{0}$ finds the corresponding $\boldsymbol{\omega}$, i.e.

$$\boldsymbol{B}_\Gamma \boldsymbol{\xi} = \boldsymbol{\omega} \quad \Leftrightarrow \quad \widehat{\boldsymbol{U}}_\Gamma^{-1}(\boldsymbol{0}, \boldsymbol{\xi}) = (\boldsymbol{\varphi}, \boldsymbol{\omega}). \tag{29}$$

The operator $\boldsymbol{B}_\Gamma$, according to [15], inherits the properties of invertibility, symmetry and positiveness of the operator $\boldsymbol{U}_\Gamma$, and the reciprocity also holds. Therefore, the task of finding the critical scales of the operator $\boldsymbol{U}_\Gamma$ or, better, $\boldsymbol{U}_{\rho\Gamma}$, is reduced to investigation of these properties for the operator $\boldsymbol{B}_{\rho\Gamma}$. According to the above definition, $\boldsymbol{B}_\Gamma$ is a second-order tensor. It should be noted that the invertibility of $\boldsymbol{U}_{\rho\Gamma}$ does not depend on whether it is applied to solve an interior or exterior BVP.

The first step in the study of $\boldsymbol{B}_{\rho\Gamma}$ will be its behaviour with respect to the scale factor $\rho$. Let us check the difference between $\boldsymbol{B}_\Gamma$ and $\boldsymbol{B}_{\rho\Gamma}$ for any $\rho > 0$.

Relation (26) for scaling $\boldsymbol{U}_{\rho\Gamma}$ renders for all $\tilde{x} \in \rho\Gamma$

$$[\boldsymbol{U}_{\rho\Gamma}\tilde{\boldsymbol{\varphi}}](\tilde{x}) = \rho\big[[\boldsymbol{M}_\rho \boldsymbol{U}_\Gamma \boldsymbol{\varphi}](\tilde{x}) - \Lambda\kappa \ln \rho \, \boldsymbol{\xi}\big]. \tag{30}$$

The vector $\boldsymbol{\xi}$ can also be scaled to $\rho\Gamma$ to obtain $\boldsymbol{\xi}_\rho$. An application of the dilation operator yields

$$\begin{aligned} \xi_{\rho k} &= \int_{\rho\Gamma} \mu_i^k(\tilde{x})[\boldsymbol{M}_\rho \boldsymbol{\varphi}]_i(\tilde{x}) \, \mathrm{d}(\rho\Gamma)(\tilde{x}) \\ &= \int_\Gamma \mu_i^k(\rho x)\varphi_i(x)\rho \, \mathrm{d}\Gamma(x) = \rho \int_\Gamma \mu_i^k(x)\varphi_i(x)\mathrm{d}\Gamma(x) = \rho\xi_k. \end{aligned} \tag{31}$$

Substituting (31) into (30), we find that

$$[\boldsymbol{U}_{\rho\Gamma}\boldsymbol{M}_\rho \boldsymbol{\varphi}](\tilde{x}) = \rho\left([\boldsymbol{M}_\rho \boldsymbol{U}_\Gamma \boldsymbol{\varphi}](\tilde{x}) - \Lambda\kappa \ln \rho \, \frac{1}{\rho}\boldsymbol{\xi}_\rho\right). \tag{32}$$

Relations (31) and (32) will be used to show the next proposition. Let $\mathbf{I}$ denote the $2 \times 2$ identity matrix.

PROPOSITION 3. *For any $\rho > 0$, we have*

$$\mathbf{B}_{\rho\Gamma} = \mathbf{B}_\Gamma - \Lambda\kappa \ln \rho \mathbf{I}. \tag{33}$$

*Proof.* Let $\boldsymbol{\varphi}$ be the solution of (28) for $\boldsymbol{g} = \boldsymbol{0}$. Then, we rewrite (32) in the matrix form

$$\begin{aligned} \boldsymbol{U}_{\rho\Gamma}\boldsymbol{M}_\rho \boldsymbol{\varphi} &= \rho \boldsymbol{M}_\rho \left(\sum_{k=1}^{2} \omega_k \boldsymbol{\mu}^k\right) - \Lambda\kappa \ln \rho \, \boldsymbol{\xi}_\rho \\ &= \rho(\boldsymbol{M}_\rho \boldsymbol{\mu}^1 \quad \boldsymbol{M}_\rho \boldsymbol{\mu}^2)\left(\boldsymbol{B}_\Gamma\left(\frac{1}{\rho}\boldsymbol{\xi}_\rho\right)\right) - \Lambda\kappa \ln \rho \, \boldsymbol{\xi}_\rho \\ &= (\boldsymbol{\mu}^1 \quad \boldsymbol{\mu}^2)\,(\boldsymbol{B}_\Gamma - \Lambda\kappa \ln \rho \, \mathbf{I})\, \boldsymbol{\xi}_\rho. \end{aligned} \tag{34}$$

The last term proves the lemma as it must be the same as (28), but now written for the scaled boundary $\rho\Gamma$ and with $\boldsymbol{g} = \boldsymbol{0}$, giving $\boldsymbol{U}_{\rho\Gamma}\tilde{\boldsymbol{\varphi}} = \sum_{k=1}^{2} \boldsymbol{\mu}^k [\boldsymbol{B}_{\rho\Gamma}\boldsymbol{\xi}_\rho]_k$. □

Finally, we may prove a theorem, which, in fact, reduces the question of invertibility of $\boldsymbol{U}_{\rho\Gamma}$ to a single eigenvalue problem for the $2 \times 2$ matrix representing $\boldsymbol{B}_\Gamma$.

THEOREM 1. *For any bounded Lipschitz boundary $\Gamma$ of a domain there exist either one or two critical scales $\rho_c$, defined by the real eigenvalues $\sigma$ of the symmetric operator $\mathbf{B}_\Gamma$ as*

$$\rho_c = \mathrm{e}^{\sigma/(\Lambda\kappa)}, \tag{35}$$

*such that the operator $\boldsymbol{U}_{\rho_c\Gamma}$ is not invertible. If there is only one critical scale, the null-space dimension of $\boldsymbol{U}_{\rho_c\Gamma}$ is two, otherwise for each particular $\rho_c$ this dimension is one.*

*Proof.* The invertibility of the operator $\boldsymbol{U}_{\rho\Gamma}$ is inherited by the operator $\boldsymbol{B}_{\rho\Gamma}$. Thus, according to Proposition 3, it is sufficient to show that equation

$$\det(\mathbf{B}_\Gamma - \Lambda\kappa \ln\rho\mathbf{I}) = 0 \tag{36}$$

has either one or two roots $\rho_c$. This is the task of finding eigenvalues $\sigma = \Lambda\kappa \ln\rho$ of the symmetric matrix representing the operator $\boldsymbol{B}_\Gamma$. Such eigenvalues $\sigma$ exist, they are always real and at most two different. The other statements of the theorem are direct consequences of Proposition 1, Lemma 2, system of equations (28) and the definition of $\boldsymbol{B}_\Gamma$ in (29). □

Definition (29), Proposition 3 and Theorem 1 enable us to find another subspace of $[H^{-1/2}(\Gamma)]^2$ where the operator $\boldsymbol{U}_\Gamma$ is not positive (cf. Lemma 1). Actually, we have proved, for each $\Gamma$, the existence of two real parameters $\rho_1 \geqslant \rho_2 > 0$, two nonzero orthogonal vectors $\boldsymbol{\xi}^1$ and $\boldsymbol{\xi}^2$ in $\mathbb{R}^2$ (eigenvectors of the symmetric operator $\boldsymbol{B}_\Gamma$) and two nonzero vector functions $\boldsymbol{\eta}^1$ and $\boldsymbol{\eta}^2$ in $[H^{-1/2}(\Gamma)]^2$ such that a special case of the system (28), with the property (31) of scaled $\boldsymbol{\xi}^k$ for $k = 1, 2$, reads

$$\boldsymbol{U}_{\rho_k\Gamma}(\boldsymbol{M}_{\rho_k}\boldsymbol{\eta}^k) = \boldsymbol{0}, \tag{37a}$$

$$\int_\Gamma \boldsymbol{\eta}^k \,\mathrm{d}\Gamma = \boldsymbol{\xi}^k. \tag{37b}$$

Hence, we may prove the following proposition.

PROPOSITION 4. *Let $\Gamma$ be a bounded Lipschitz boundary of a domain. Let $\rho_k$ ($\rho_1 \geqslant \rho_2$) and $\boldsymbol{\xi}^k$ with $\boldsymbol{\eta}^k$ be as specified in* (37). *Then for each $\rho < \rho_2$ the operator $\boldsymbol{U}_{\rho\Gamma}$ is positive in $[H^{-1/2}(\rho\Gamma)]^2$, for each $\rho > \rho_1$ the operator $\boldsymbol{U}_{\rho\Gamma}$ is negative in a two-dimensional subspace of $[H^{-1/2}(\rho\Gamma)]^2$ defined by the basis $\boldsymbol{M}_\rho\boldsymbol{\eta}^1$ and $\boldsymbol{M}_\rho\boldsymbol{\eta}^2$, and finally, when $\rho_1 > \rho_2$, for $\rho$ between $\rho_1$ and $\rho_2$ the operator $\boldsymbol{U}_{\rho\Gamma}$ is negative in a one-dimensional subspace defined by $\boldsymbol{M}_\rho\boldsymbol{\eta}^2$.*

*Proof.* Let $\boldsymbol{\varphi} \in [H^{-1/2}(\Gamma)]^2$. Then, $\boldsymbol{\varphi}$ can be uniquely split to $\boldsymbol{\varphi} = \hat{\boldsymbol{\varphi}} + \alpha_1\boldsymbol{\eta}^1 + \alpha_2\boldsymbol{\eta}^2$, with $\hat{\boldsymbol{\varphi}}$ satisfying the condition $\int_\Gamma \hat{\boldsymbol{\varphi}}\,\mathrm{d}\Gamma = \mathbf{0}$. Taking into account that $\boldsymbol{U}_\Gamma\boldsymbol{\eta}^s = \Lambda\kappa \ln\rho^s\boldsymbol{\xi}^s$ due to (32) and (37a), it is easy to see that

$$\begin{aligned}
&\int_{\rho\Gamma} (\boldsymbol{M}_\rho\boldsymbol{\eta}^r)_i \big[\boldsymbol{U}_{\rho\Gamma}(\boldsymbol{M}_\rho\boldsymbol{\eta}^s)\big]_i\,\mathrm{d}(\rho\Gamma)\\
&\quad= \rho^2\int_\Gamma \eta_i^r\left[[\boldsymbol{U}_\Gamma\boldsymbol{\eta}^s]_i - \Lambda\kappa\ln\rho\int_\Gamma \eta_i^s\,\mathrm{d}\Gamma\right]\mathrm{d}\Gamma\\
&\quad= \rho^2\int_\Gamma \eta_i^r\left[\Lambda\kappa\ln\frac{\rho^s}{\rho}\boldsymbol{\xi}^s\right]_i\mathrm{d}\Gamma = \rho^2\Lambda\kappa\ln\frac{\rho^s}{\rho}\,\xi_i^s\xi_i^r,
\end{aligned} \tag{38}$$

where $\xi_i^s\xi_i^r$ can be taken as $\delta_{rs}$. Similar reasoning leads to the identity

$$\int_{\rho\Gamma} (\boldsymbol{M}_\rho\hat{\boldsymbol{\varphi}})_i \big[\boldsymbol{U}_{\rho\Gamma}(\boldsymbol{M}_\rho\boldsymbol{\eta}^s)\big]_i\mathrm{d}(\rho\Gamma) = \rho^2\int_\Gamma \hat{\varphi}_i\left[\Lambda\kappa\ln\frac{\rho^s}{\rho}\boldsymbol{\xi}^s\right]_i\mathrm{d}\Gamma = 0. \tag{39}$$

These relations together with Proposition 1 prove the proposition. □

Unfortunately, this proposition is of small practical usage, because the functions $\boldsymbol{\eta}^k$ are not known a priori and generally are quite complicated. Also the critical scales are not easily found. In the simplest case of a circular domain, however, as shown in [20, 21], $\boldsymbol{\eta}^k$ are equal to $\boldsymbol{\mu}^k$ so that Lemma 1 and Proposition 4 deal with the same subspaces.

Finally, let us mention that Theorem 1 and Proposition 4 confirm previous analytical and numerical studies by Heise and co-workers [20, 21, 26] of some particular cases.

### 3.3. BOUNDED MULTIPLY CONNECTED DOMAIN

Let us study the critical scales of a bounded multiply connected domain. The boundary $\Gamma$ of such a domain, see (2), always contains an external border $\Gamma_0$, which plays an important role in finding the critical scales of this domain. The next proposition specifies this role.

PROPOSITION 5. *Let $\Gamma$ be a Lipschitz boundary of a bounded multiply connected domain with an external boundary $\Gamma_0 \subset \Gamma$. Then $\rho_c$ is a critical scale factor of $\Gamma$ iff it is a critical scale factor of $\Gamma_0$.*

*Proof.* Let $\rho_c$ be a critical scale of $\Gamma_0$. Then there exists $\boldsymbol{\varphi} \in [H^{-1/2}(\rho_c\Gamma_0)]^2$ such that $\boldsymbol{U}_{\rho_c\Gamma_0}\boldsymbol{\varphi} = \mathbf{0}$. Let $\widetilde{\boldsymbol{U}}\boldsymbol{\varphi}$ denote the associated single-layer potential. Thus, $\boldsymbol{u}_\varphi = \widetilde{\boldsymbol{U}}\boldsymbol{\varphi}$ is the unique solution of the interior Dirichlet BVP in $\rho_c$ scaled $\Omega_0$ with zero boundary conditions at $\rho_c\Gamma_0$. Hence, $\boldsymbol{u}_\varphi = \mathbf{0}$ in scaled $\Omega_0$. Now, let us take a function $\tilde{\boldsymbol{\varphi}} \in [H^{-1/2}(\rho_c\Gamma)]^2$, which is equal to $\boldsymbol{\varphi}$ on $\rho_c\Gamma_0$ and zero elsewhere on $\rho_c\Gamma$. Then

$$\begin{aligned}
&x \in \rho_c\Gamma_0: && (\boldsymbol{U}_{\rho_c\Gamma}\tilde{\boldsymbol{\varphi}})(x) = (\boldsymbol{U}_{\rho_c\Gamma_0}\boldsymbol{\varphi})(x) = \mathbf{0},\\
&x \in \rho_c\Gamma \setminus \rho_c\Gamma_0: && (\boldsymbol{U}_{\rho_c\Gamma}\tilde{\boldsymbol{\varphi}})(x) = (\widetilde{\boldsymbol{U}}\boldsymbol{\varphi})(x) = \mathbf{0}.
\end{aligned} \tag{40}$$

Therefore, $\tilde{\boldsymbol{\varphi}}$ is in the null-space of $\boldsymbol{U}_{\rho_c\Gamma}$, implying $\rho_c$ is a critical scale of $\Gamma$. The proof is easily completed by virtue of Theorem 1. □

Notice, that the above proof specifies the null-space of $\boldsymbol{U}_{\rho_c\Gamma}$ for a bounded multiply connected domain and shows that it is independent of the number and forms of holes.

### 3.4. OTHER FUNDAMENTAL SOLUTIONS

So far, we have analysed what happens if the domain is scaled, e.g., by changing the unit of length. Another possibility of changing and controlling the critical scales is to choose the integral kernel of the operator $\boldsymbol{U}_\Gamma$, i.e. a fundamental solution of Navier equation (2a). It is well known, lacking any vanishing condition at infinity in two-dimensional elasticity, that $U_{ij}$ in (6) can be changed by an arbitrary constant, so it is possible to apply a modified integral kernel $U^\varsigma_{ij} = U_{ij} + \Lambda\kappa \ln\varsigma\, \delta_{ij}$ and, subsequently, modified single-layer potential

$$\boldsymbol{U}^\varsigma_\Gamma\boldsymbol{\varphi} = \boldsymbol{U}_\Gamma\boldsymbol{\varphi} + \Lambda\kappa \ln\varsigma \int_\Gamma \boldsymbol{\varphi}\, \mathrm{d}\Gamma. \tag{41}$$

It is obvious that Proposition 1 and Lemma 1 are not altered by a change of $\varsigma$. Nevertheless, it may be useful to know how the radius $R$ in Proposition 2 and the operator $\boldsymbol{B}_\Gamma$ are modified.

Substituting (41) into (23) leads, in view of $\int_\Gamma \varphi_k \mathrm{d}\Gamma = c_k$, to

$$\int_\Gamma \varphi_i [\boldsymbol{U}^\varsigma_\Gamma\boldsymbol{\varphi}]_i \,\mathrm{d}\Gamma > \frac{\Lambda}{2}\left(-2\kappa \ln\frac{R}{\varsigma} + 1\right)(c_1^2 + c_2^2). \tag{42}$$

The right-hand side vanishes if $(-2\kappa \ln(R/\varsigma) + 1) = 0$ thus $R$ in Proposition 2 converts to $R/\varsigma$.

Similarly, substituting (41) into (28a) with $\boldsymbol{g} = \boldsymbol{0}$, we obtain

$$\boldsymbol{U}^\varsigma_\Gamma\boldsymbol{\varphi} = \sum_{k=1}^{2} \omega_k \boldsymbol{\mu}^k + \Lambda\kappa \ln\varsigma\, \boldsymbol{\xi} = \sum_{k=1}^{2} \omega^\varsigma_k \boldsymbol{\mu}^k. \tag{43}$$

Applying definitions of $\boldsymbol{B}_\Gamma$ and $\boldsymbol{B}^\varsigma_\Gamma$ to (43) renders

$$\begin{aligned} 0 &= \sum_{k=1}^{2} \left(\omega_k - \omega^\varsigma_k\right) \boldsymbol{\mu}^k + \Lambda\kappa \ln\varsigma\, \boldsymbol{\xi} = \boldsymbol{B}_\Gamma\boldsymbol{\xi} - \boldsymbol{B}^\varsigma_\Gamma\boldsymbol{\xi} + \Lambda\kappa \ln\varsigma\, \boldsymbol{\xi} \\ &= (\boldsymbol{B}_\Gamma - \boldsymbol{B}^\varsigma_\Gamma + \Lambda\kappa \ln\varsigma \mathbf{I})\boldsymbol{\xi}, \end{aligned} \tag{44}$$

and finally,

$$\boldsymbol{B}^\varsigma_\Gamma = \boldsymbol{B}_\Gamma + \Lambda\kappa \ln\varsigma \mathbf{I}. \tag{45}$$

Both, Proposition 3 and Theorem 1, therefore remain valid also for the modified single-layer operator $\boldsymbol{U}_\Gamma^\varsigma$.

An application of the integral kernel $U_{ij}^\varsigma$ thus introduces another approach to guarantee the single-layer operator to be invertible for a particular $\Gamma$, being sufficient that $\Gamma$ is contained in a disk of radius $R = \varsigma \mathrm{e}^{1/(2\kappa)}$.

## 4. Examples

Several examples have been chosen to cover various types of domains. The solution of the first example – a rigid line inclusion – is analytic, whereas numerical solutions are presented for the others examples. Our attention is focused on calculation of critical scale factors $\rho_c$ for each geometrical form. In all present calculations the unmodified single-layer potential introduced in (6) and the associated single-layer boundary integral operator. $\boldsymbol{U}_\Gamma$ have been used. Evaluation of critical scales starts in the next numerical examples with a numerical solution of the system (28) with $\boldsymbol{g} = \boldsymbol{0}$ for two linearly independent choices of $\boldsymbol{\xi}$. The solutions obtained enable us to find an approximation of the matrix $\boldsymbol{B}_\Gamma$ for a particular scale, no necessarily a critical one. Finally, using Theorem 1 the critical scales $\rho_c$ are calculated solving the eigenvalue problem for $\boldsymbol{B}_\Gamma$.

The following geometries are considered: a rectangular region, an elliptic region, an infinite plane with two circular holes and a bounded rectangular region with two rectangular holes. For simplicity, in all problems studied the material parameters are chosen as follows: the shear modulus $G$ is equal to unity and the Poisson ratio $\nu$ is equal to a quarter, if not stated otherwise.

An SGBEM code, with continuous straight linear elements and analytic integrations, has been used to solve numerically (28). The BEM meshes applied have been either uniform, along all straight and circular parts of boundaries, or naturally quasi-uniform, along elliptic boundaries. The number of elements is kept constant in each particular example when the domain is scaled.

### 4.1. RIGID LINE INCLUSION, AN ANALYTICAL SOLUTION

First, let us consider the problem of a rigid line inclusion of length $2L$ as shown in Figure 3. Thus, elastic domain $\Omega = \mathbb{R}^2 \setminus (\langle -L, L\rangle \times \{0\})$. This geometry represents, although the boundary $\Gamma$ is not Lipschitz ($\Omega$ not being locally on one side of $\Gamma$), a limit state of geometries in the two following examples.

Critical scales of such an inclusion can be calculated analytically, using the complex potentials of Kolosoff–Muskhelishvili [27]. These scales are defined by the nontrivial solutions of the exterior problem with vanishing displacements at the rigid line inclusion and satisfying the radiation condition (8), which in complex

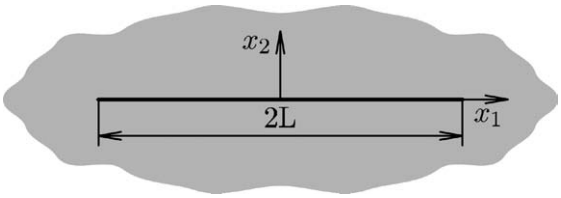


*Figure 3.* Rigid line inclusion geometry.

variable notation has the form:

$$u_1(z) + \mathrm{i}u_2(z) = \frac{\Lambda}{2}\left[b(-2\kappa \ln r + 1) + \overline{b}\,\frac{z}{\overline{z}}\right] + \mathrm{O}(r^{-1}), \quad r \to \infty, \tag{46}$$

with $b = b_1 + \mathrm{i}b_2$ and $z = x_1 + \mathrm{i}x_2 = r\mathrm{e}^{\mathrm{i}\vartheta}$. To satisfy this condition, let us define the potential functions $\phi$ and $\psi$ as follows:

$$\begin{aligned} \phi(z) &= A \ln \frac{1}{2}(z^2 + \sqrt{z^2 - L^2}), \\ \psi(z) &= \bar{A}\left(1 - \kappa \ln \frac{1}{2}\left(z^2 + \sqrt{z^2 - L^2}\right)\right) + A\left(1 - \frac{z}{\sqrt{z^2 - L^2}}\right), \end{aligned} \tag{47}$$

where $A$ is a complex constant $A = A_1 + \mathrm{i}A_2$ and

$$\ln z = \ln r + \mathrm{i}\vartheta, \quad \vartheta \in (-\pi, \pi), \tag{48}$$

$$\sqrt{z^2 - L^2} = \zeta \quad \Leftrightarrow \quad (z^2 = \zeta^2 + L^2 \wedge |z + \zeta| > |z - \zeta|). \tag{49}$$

The displacements of the points out of the inclusion can be expressed, using the potential functions as

$$\begin{aligned} &2\mu(u_1(z) + \mathrm{i}u_2(z)) \\ &\quad = \kappa\phi(z) - z\overline{\phi'(z)} - \overline{\psi(z)} \\ &\quad = 2\left(A\kappa \ln\left(\frac{1}{2}\left|z + \sqrt{z^2 - L^2}\right|\right) - \Re A - \frac{\mathrm{i}\bar{A}}{\sqrt{z^2 - L^2}}\,\Im z\right), \end{aligned} \tag{50}$$

where $\Re$ and $\Im$ respectively denote the real and imaginary parts of a complex number. When $z$ approaches the inclusion, this relation becomes

$$2\mu(u_1(z) + \mathrm{i}u_2(z))\big|_{\substack{z = x_1 \pm \mathrm{i}0 \\ |x_1| \leqslant L}} = 2\left(A\kappa \ln \frac{L}{2} - \Re A\right), \tag{51}$$

which produces zero displacements at boundary only when the following conditions are satisfied:

$$\begin{aligned} &2\mu(u_1(z) + \mathrm{i}u_2(z))\big|_{\substack{z = x_1 \pm \mathrm{i}0 \\ |x_1| \leqslant L}} = 0 \\ &\quad \Leftrightarrow \quad \left(A_2 = 0 \wedge L = 2\mathrm{e}^{1/\kappa}\right) \vee (A_1 = 0 \wedge L = 2). \end{aligned} \tag{52}$$

Hence, we conclude that a rigid line inclusion has in accordance with Theorem 1 two critical scales. One of them is independent of material properties and causes an inclusion of length four (in the used unit of length) to be critical. The other depends on the material and the corresponding inclusion length is $4e^{1/\kappa}$. Notice, that the positivity guess of Proposition 2 guarantees that for any inclusion of length less than $2e^{1/2\kappa}$ the operator $\boldsymbol{U}_\Gamma$ is positive, though in fact it is positive for any line inclusion of length less than four due to Lemma 4.

### 4.2. RECTANGLE

The first numerical example deals with a rectangular domain, see Figure 4. The shape of the domain is changed during the present parametric study in the following way: the length of one side is kept fixed at unity, the other side length varies between zero and unity. This allows us to find the critical scales for any rectangular domain.

The critical scales calculated for a series of BEM meshes with 40 elements along each rectangular boundary are shown in Figure 5. These scales coincide in

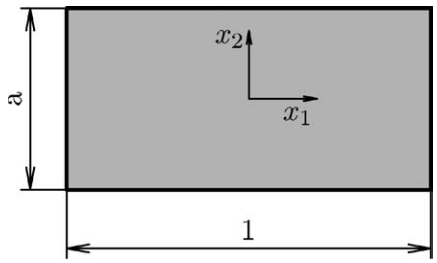


*Figure 4.* Rectangle geometry.

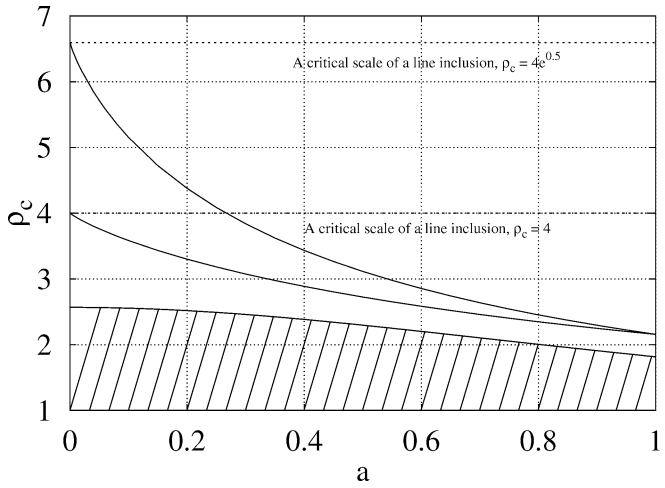


*Figure 5.* Critical scales – rectangle.

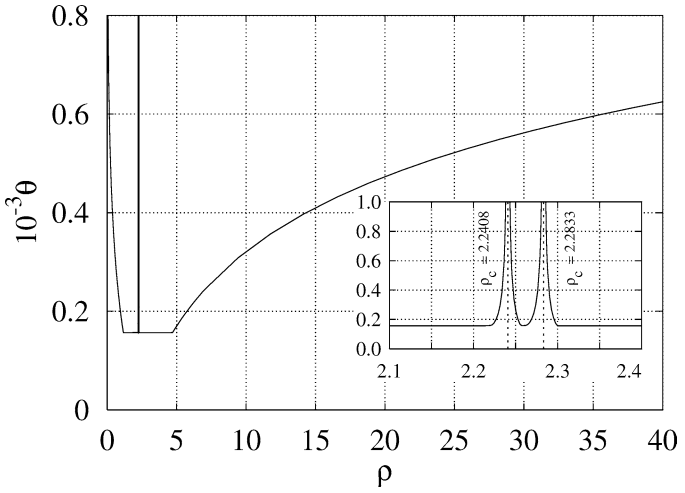


*Figure 6.* Condition numbers – rectangle, $a = 10/11$.

the case of a square ($a = 1$, $\rho_c = 2.156944$) and approach the critical scales of a rigid line inclusion, when $a$ is sufficiently small. We can also show an estimate of the domain size, for which the positiveness of $\boldsymbol{U}_\Gamma$ is guaranteed according to Proposition 2. The radius of the circumscribed circle of $\rho\Gamma$ equals $\frac{1}{2}\rho\sqrt{1+a^2}$. The hatched area of Figure 5 shows the zone of all $\rho$ for which this radius is less than $\mathrm{e}^{1/(2\kappa)}$ for every $a$. It is obviously situated below both curves of $\rho_c$. The picture also documents how efficient is the estimate because, due to Proposition 4, $\boldsymbol{U}_\Gamma$ is positive for all points below the bottom curve of $\rho_c$.

The critical scale of a domain causes the integral equation operator $\boldsymbol{U}_\Gamma$ to have a nontrivial null-space. However, the behaviour of the operator spectrum near this critical scale is also very important. We can study this spectrum numerically, analysing the spectrum of the SGBEM discretisation matrix.

Let us look at the numerical results obtained for a particular value $a = 10/11$ and a uniform mesh with 11 elements on the longer side and 10 on the shorter side of the rectangle. Figure 6 shows the condition number $\theta$ of the SGBEM discretisation matrix:

$$\theta, = \frac{\sigma_{\max}}{\sigma_{\min}}, \tag{53}$$

$\sigma_{\max}$ and $\sigma_{\min}$ being respectively maximum and minimum singular values, as a function of the scaling factor $\rho$. It is clear that near the critical scales $\theta$ tends to infinity. The dashed lines correspond to the critical scales 2.240785, 2.283305 calculated according to (35). Both values, of course, coincide with the peaks of the condition number. The condition number also tends to infinity as $\rho$ approaches zero or infinity, the approximate behaviour in both cases is $\mathrm{O}(\ln \rho)$. Within an interval of $\rho$, as is clearly seen in Figure 6, $\theta$ is almost constant except for a small vicinity of $\rho_c$. This observation is in clear agreement with results in [21] and also

*Table I.* Convergence rates for the rectangle $a = 10/11$

| $N$ | $\rho_1$ | $\rho_2$ | $\alpha_1$ | $\tilde{\rho}_1$ | $\alpha_2$ | $\tilde{\rho}_2$ |
|---|---|---|---|---|---|---|
| 22 | 2.242867 | 2.285450 | | | | |
| 42 | 2.240785 | 2.283305 | | | | |
| 84 | 2.239813 | 2.282303 | 1.247 | 2.239105 | 1.247 | 2.281574 |
| 168 | 2.239398 | 2.281876 | 1.229 | 2.239089 | 1.228 | 2.281558 |
| 336 | 2.239221 | 2.281693 | 1.224 | 2.239088 | 1.224 | 2.281556 |

in [6, 8]. Studies of eigenvalues of $\boldsymbol{U}_\Gamma$ for the circular disk [20, 21, 26] and also for an irregular slice [26] show that only two eigenvalues, which cause critical scales, depend nonlinearly on the domain size. Thus, the observed approximately constant condition number is caused by a linear and homogeneous variation of the rest of the eigenvalues during scaling. These facts also explain the logarithmic behaviour of $\theta$ near zero and at infinity.

In order to estimate the accuracy of the numerical results presented the following convergency test has been carried out. Various uniform meshes (except for the first one – 6 and 5 elements respectively placed along the longer and shorter sides) were used to calculate the critical scales in Table I. The second mesh is the same as used in Figure 6. Convergence rates $\alpha_m$ ($m = 1, 2$) and the extrapolated critical scales $\tilde{\rho}_m$ were calculated using a three-parameter fit function $\rho_m = \tilde{\rho}_m + K\, N^{-\alpha}$. The parameters were at each instance calculated from three previous approximations of $\rho_m$. Thus, the last values in the fifth and the seventh column should have errors about $10^{-6}$. The convergence rates are about a quarter higher than unity, this relatively low rate being caused by the non-smooth (rectangular) boundary including corners. A small shift between the critical scales associated to a coarse and a fine mesh can be observed in Figure 7, where the condition numbers $\theta$ (in fact $\theta/N$ is presented to eliminate the linear dependence of $\theta$ on $N$) of the discretisation matrices associated to the meshes with $N$ being 42 and 168 are plotted. The vertical lines are placed at the calculated critical scales $\rho_c$ given in the corresponding rows of Table I. Note that, apart from the shift of the calculated critical scales for the refined mesh, a narrower interval of $\rho$ around each critical scale, where the condition numbers $\theta$ present a singular behaviour, appears for this mesh.

### 4.3. ELLIPSE

Critical scales of an elliptic domain, see Figure 8, are evaluated in this example.

The shape of the domain is changed to find the critical scales for any ellipse: the length of one semi-axis is kept fixed at unity, the other semi-axis length varies between zero and unity. Each elliptic boundary is discretised by a quasi-uniform mesh with 40 elements.

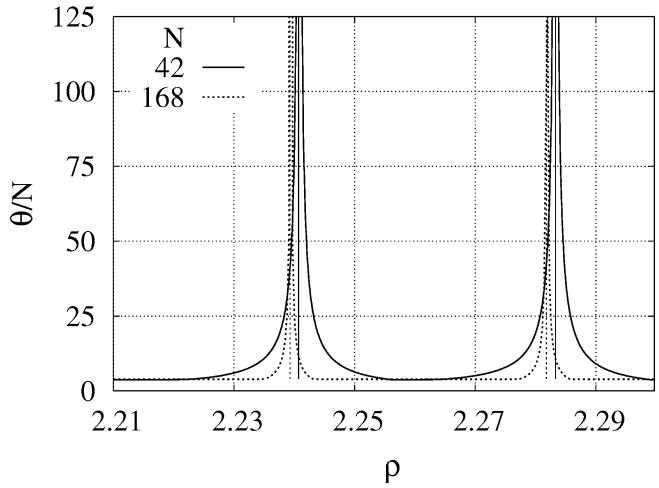


*Figure 7.* Condition numbers, rectangle $a = 10/11$, a comparison of two meshes around the critical scales.

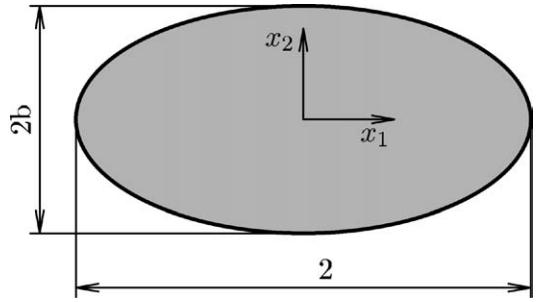


*Figure 8.* Ellipse geometry.

The two critical scales as a function of $b$ are shown in Figure 9. These scales coincide in the case of a circle ($b = 1$, $\rho_c = \mathrm{e}^{1/4}$ [11]) and are approaching the critical scales of a line inclusion, when $b$ is very small. The positiveness of $\boldsymbol{U}_\Gamma$ is guaranteed by Proposition 2 in the hatched area, whose extent is clear considering the radius of the circumscribed circle of $\rho\Gamma$ is equal to $\rho$. Thus, the efficiency of the estimate, as contrasted with Proposition 4, which guarantees $\boldsymbol{U}_\Gamma$ to be positive for all scales below the bottom curve of $\rho_c$, can be observed. In particular, the guess is the best one for a circle, due to the proof of Proposition 2.

A sufficient accuracy seems to be achieved for rather coarse meshes when comparing with the convergence study for a rectangle. Results for an ellipse with $b = 1/2$ discretised by five meshes are shown in Table II. As could be expected due to the smooth character of the elliptic boundary, the rates of convergence obtained are close to two. The claim about the accuracy is also supported by the results obtained for the unit circle, whose critical scale evaluated analytically is

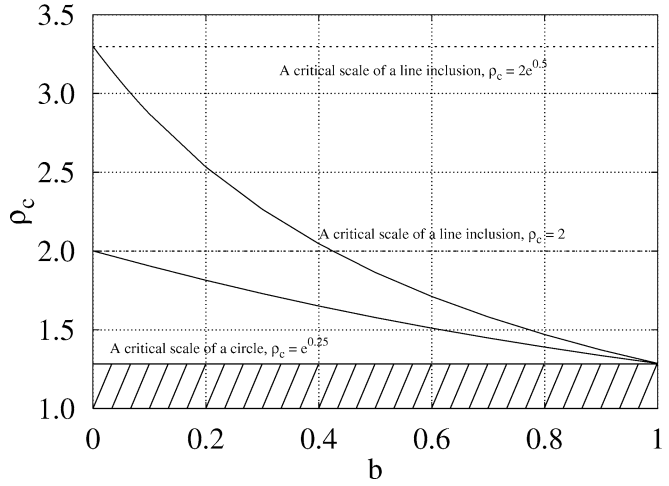


*Figure 9.* Critical scales – ellipse, $\nu = 0.25$.

*Table II.* Convergence rates for the ellipse $b = 1/2$

| $N$ | $\rho_1$ | $\rho_2$ | $\alpha_1$ | $\tilde{\rho}_1$ | $\alpha_2$ | $\tilde{\rho}_2$ |
|---|---|---|---|---|---|---|
| 6 | 1.695534 | 2.032902 | | | | |
| 12 | 1.608920 | 1.902459 | | | | |
| 24 | 1.583873 | 1.871284 | 1.790 | 1.573683 | 2.065 | 1.861494 |
| 48 | 1.577363 | 1.863451 | 1.944 | 1.575076 | 1.993 | 1.860823 |
| 96 | 1.575705 | 1.861478 | 1.974 | 1.575139 | 1.989 | 1.860813 |

$\rho_c = \mathrm{e}^{0.25} = 1.284025$ and the best extrapolated numerical result (obtained by meshes with the same number of elements as used for ellipse) is 1.284023.

Figure 10 shows how $\rho_c$ depend on $\nu$, varying $\nu$ within its limits for common isotropic materials. Each curve corresponds to a particular value of the parameter $b$ (small numbers near each curve). In the left part of the figure the lower critical scales are presented. It is clear that, for vanishing $b$, $\rho_c$ approach value two, independently of $\nu$. While the greater critical scales, shown in the right part of the figure, approach for vanishing $b$, according to Section 4.1, the following limit curve: $\rho_c = 2\mathrm{e}^{1/(3-4\nu)}$ – the dashed line. Notice, that the bottom limit curves (theoretically $\rho_c = \mathrm{e}^{1/(2(3-4\nu))}$, represented by the almost hidden dashed lines) on the left and right figure parts, associated to the circle, are in fact the same. Moreover, they coincide with the boundary curve of the hatched domain – the region where $\boldsymbol{U}_\Gamma$ is positive following an estimate by Proposition 2.

The above numerical results agree with analytical results deduced in [4], where, however, $\boldsymbol{U}_\Gamma^\varsigma$ is used with $\varsigma = \mathrm{e}^{-1/2(3-4\nu)}$. The critical radius of a circular disk is in this case equal to unity, see Section 3.4.

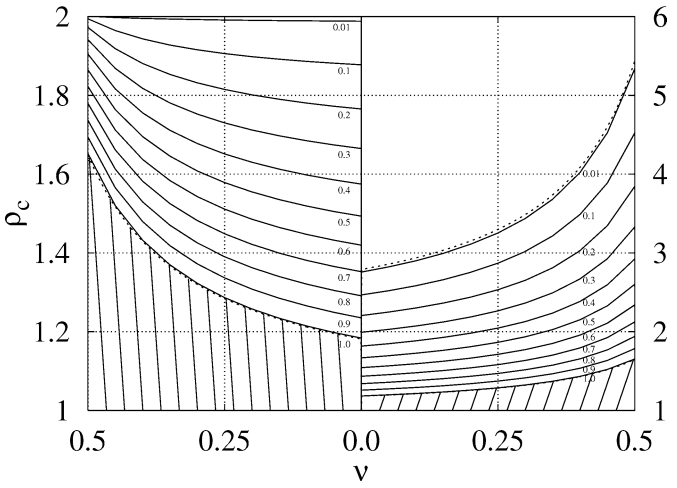


*Figure 10.* Critical scales as functions of the Poisson ratio $\nu$ for ellipse.

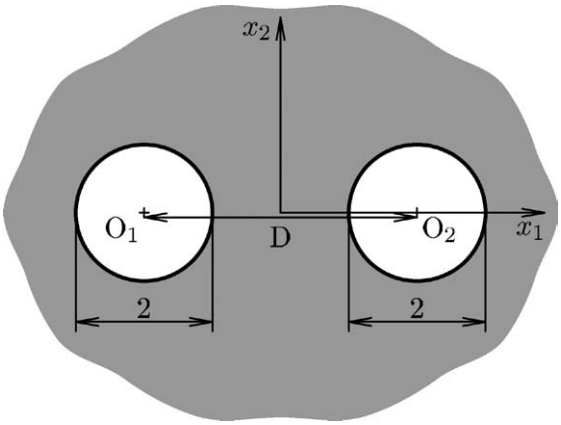


*Figure 11.* Two circular holes, geometry description.

### 4.4. TWO CIRCULAR HOLES

Let $\Omega$ be defined as an exterior domain to two circular holes, see Figure 11. The basic configuration consists of two circles with the unit radii, which centers are placed at a distance $D > 2$. Relation between $\rho_c$ and the geometry parameter $D$ is analysed, the obtained results being shown in Figure 12. Uniform BEM meshes with 40 elements placed on each contour have been applied. It appears that for large $D$ both $\rho_c$ behave as $\mathrm{O}(D^{-1/2})$, see the detail picture using log–log scales in Figure 12 (the dashed line represents the function $1.3D^{-0.5}$). The area, where the positivity of $\boldsymbol{U}_\Gamma$ is guaranteed by Proposition 2, is hatched again. The radius of the circumscribed circle of $\rho\Gamma$ equals $\frac{1}{2}\rho(D+2)$. Therefore, for $D$ tending to infinity, the bound provided by Proposition 2 behaves as $\mathrm{O}(D^{-1})$, having then significantly lower values than $\rho_c$ with observed $\mathrm{O}(D^{-1/2})$ behaviour.

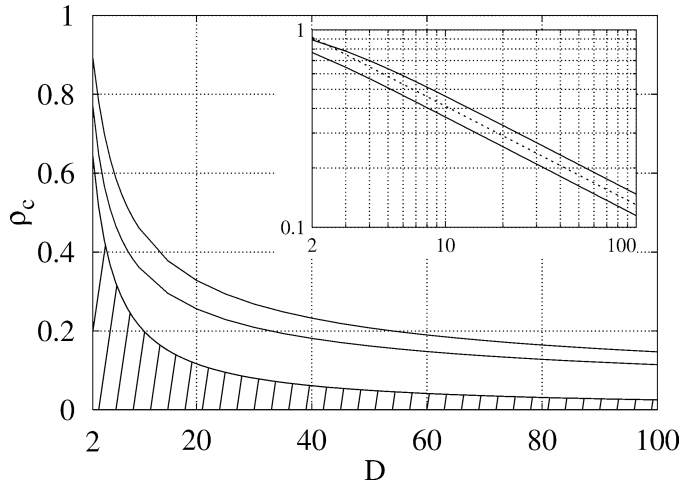


*Figure 12.* Critical scales – two circles.

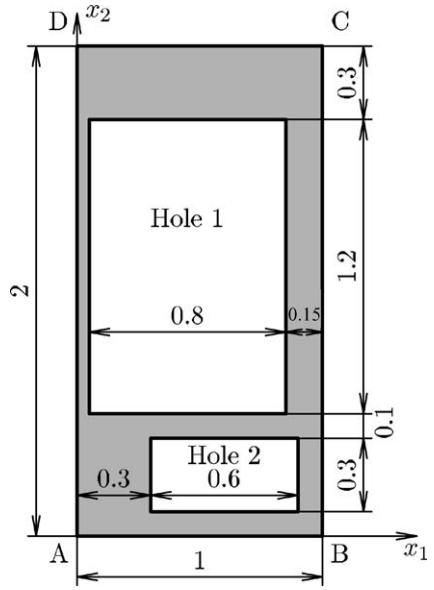


*Figure 13.* Bounded domain with rectangular holes, geometry description.

## 4.5. BOUNDED DOMAIN WITH TWO RECTANGULAR HOLES

A multiply connected domain with non-smooth outer and also hole boundaries is analysed, see Figure 13 for its basic configuration. A uniform BEM mesh with 118 elements has been applied. Applying (35) the following critical scales: 1.362790 and 1.557598 have been obtained. Another possibility how to find these scales is to calculate the condition numbers $\theta$ according to (53) for various scale factors $\rho$. The relation between the results obtained by these two approaches is studied in Fig-

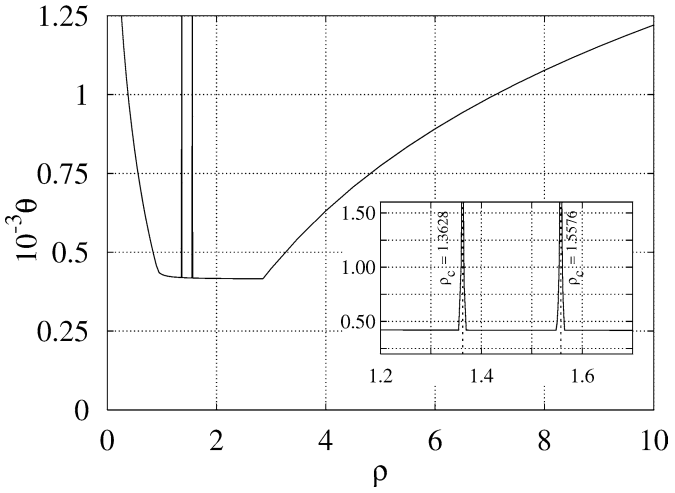


*Figure 14.* Condition numbers – bounded domain with rectangular holes.

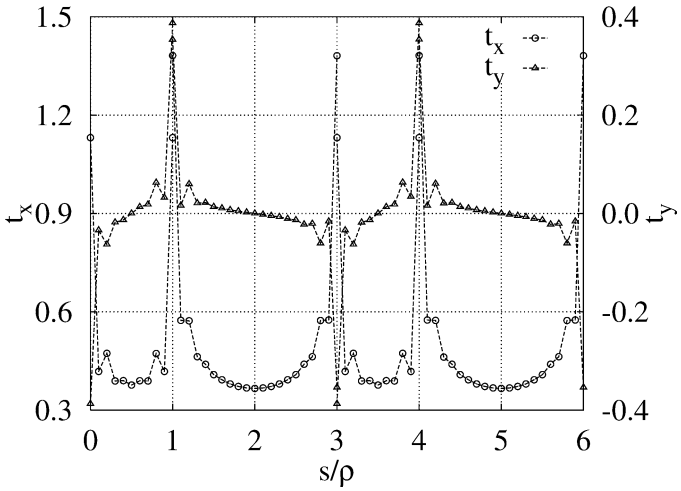


*Figure 15.* SGBEM approximation of the zero eigen-solution at the critical scale $\rho_c = 1.362790$.

ure 14. As expected, in view of results in Section 4.2, $\theta$ behaves as $O(\ln \rho)$ for large and small $\rho$. Two singularities in $\theta$ appear within the zone of approximately constant $\theta$. The positions of these singularities, see the detail picture, confirm the values of $\rho_c$ predicted by (35).

Let us recall, that due to Proposition 5, a critical scale for the multi-connected domain analysed equals, in fact, a critical scale of the outer rectangle (compare with Figure 5), the zero eigen-solution for the whole multi-connected domain being equal to that of the outer rectangle and vanishing on the holes. An SGBEM approximation of the zero eigen-solution belonging to the lower critical scale is plotted, naturally along the outer boundary only starting from the point A, in Figure 15.

Note, that the singular behaviour observed at the sharp corners of the outer rectangle corresponds to the following facts, first this zero eigen-solution is actually equal to a traction solution of an exterior problem with the boundary defined by the outer rectangle, and second such a traction solution is singular at the re-entrant corners of the exterior domain [18].

## 5. Concluding Remarks

The problem of determination of critical scales associated to a two-dimensional boundary $\Gamma$, for which the isotropic elastic single-layer potential operator $\boldsymbol{U}_\Gamma$ is not invertible, has been studied. The well-known concept of the Robin constant associated to $\Gamma$ in the potential theory has been generalized to isotropic elasticity introducing a symmetric second-order tensor $\boldsymbol{B}_\Gamma \in \mathbb{R}^{2\times 2}$ and deducing a formula for scaling this tensor (33). The relation between the tensors $\boldsymbol{B}_\Gamma$ associated to different definitions of the fundamental solution of Navier equation has been established. It has been shown that eigenvalues of $\boldsymbol{B}_\Gamma$ define through expression (35) either two single critical scales $\rho_1 > \rho_2$ (the dimension of the null-space of $\boldsymbol{U}_\Gamma$ is one) or one double critical scale $\rho_1 = \rho_2$ (the dimension is two now) of $\Gamma$. The critical scales of a bounded multiply-connected domain are equal to the critical scales of the outer boundary contour. In view of the tensor character of $\boldsymbol{B}_\Gamma$, the critical scales of a boundary $\Gamma$ are independent of its orientation with respect to the Cartesian coordinate system. It can easily be shown that a boundary $\Gamma$ with a symmetry-transformation group including a rotation by an angle different from $k\pi$ ($k$ an integer), has associated one double critical scale. This is the case, for example, of any regular polygon or circle.

It can be useful to know that single-layer potential operator $\boldsymbol{U}_{\rho\Gamma}$ defined on the scaled boundary $\rho\Gamma$ is positive for $\rho < \rho_2$ and has two negative eigenvalues for $\rho > \rho_1$. A bound for the radius $R$ of the circumscribed circle of $\Gamma$ which guarantees the positivity and thus invertibility of $\boldsymbol{U}_\Gamma$ can be given for each form of the fundamental solution, see Section 3.4. Whereas for the fundamental solution usually used in BEM (4), this bound is a function of the Poisson ratio $\nu$, having the form $R < \mathrm{e}^{1/2\kappa}$ and its value being 1.074041 for $\nu = -1$ and 1.648721 for $\nu = 0.5$, for the fundamental solution used in [11] this bound is independent of $\nu$, its value being $\mathrm{e}^{-1} = 0.367879$.

Analytical and numerical examples presented have confirmed and illustrated the conclusions of the theory developed. In particular, it has been verified that the boundary sizes, for which singularities in the condition number of the discretised version of $\boldsymbol{U}_\Gamma$ take place, coincide with those predicted, by the above mentioned formula, as critical.

Although in the present study only plane strain state has been considered, the results obtained are directly applicable to plane stress state by the pertinent modification of material constants.

It should be mentioned, that the theoretical results presented in Section 3 could also be formulated working with the subspace of all rigid body motions, instead of the subspace of rigid body translations, as has been done for the purpose of simplicity here. In this way, a matrix defined by Constanda [11] (see Theorem 2 therein) would directly correspond to the symmetric tensor $\widetilde{\mathbf{B}}_\Gamma \in \mathbb{R}^{3\times 3}$ defined according to Lemma 2. Let us present, for the completeness purposes, the formula (analogous to (33)) for scaling this tensor

$$\widetilde{\mathbf{B}}_{\rho\Gamma} = \mathbf{D}_\rho\big(\widetilde{\mathbf{B}}_\Gamma - \Lambda\kappa \ln \rho\mathbf{J}\big)\mathbf{D}_\rho,$$

where $\mathbf{D}_\rho$ and $\mathbf{J}$ are diagonal matrices defined as

$$\mathbf{D}_\rho = \operatorname{diag}\big[1,\ 1,\ \rho^{-1}\big] \quad \text{and} \quad \mathbf{J} = \operatorname{diag}[1,\ 1,\ 0].$$

Note that $\widetilde{\mathbf{B}}_\Gamma$ does not vanish for any boundary $\Gamma$, whereas $\mathbf{B}_\Gamma$ can be zero, what happens, for example, for the circle of radius $\mathrm{e}^{1/2\kappa}$ when the fundamental solution from (4) is considered.

Finally, it is considered that the present work has established a sound theoretical basis for subsequent development of general methods for removing of non-uniqueness in the numerical solution of BIE's (in the spirit of methods developed in [1, 29]), which will take into account the phenomenon of critical sizes in two-dimensional elastic problems.

## Acknowledgement

This work was originated while the first author was on a research stay at the University of Seville supported by the Junta de Andalucía. The authors are indebt to Prof. F. París of the University of Seville for comments which helped to improve the paper and the stimulating environment he provided. The authors acknowledge the financial support from the Scientific Grant Agency of the Slovak Republic (Grant No. 1/8033/01) given to R.V. and from the Spanish Ministry of Science and Technology (Project No. MAT2000-1115) given to V.M.

## References

1. A. Blázquez, V. Mantič, F. París and J. Cañas, On the removal of rigid body motions in the solution of elastostatic problems by direct BEM. *Internat. J. Numer. Methods Engrg.* **39** (1996) 4021–4038.
2. M. Bonnet, G. Maier and C. Polizzotto, Symmetric Galerkin boundary element method, *Appl. Mech. Rev.* **15** (1998) 669–704.
3. G. Chen and J. Zhou, *Boundary Element Methods*. Academic Press, London (1992).
4. J.T. Chen, S.R. Kuo and J.H. Lin, Analytical study and numerical experiments for degenerate scale problems in the boundary element method for two-dimensional elasticity. *Internat. J. Numer. Methods Engrg.* **54** (2002) 1669–1681.
5. J.T. Chen, C. Lee, I.L. Chen and J.H. Lin, An alternative method for degenerate scale problems in boundary element method for the two-dimensional Laplace equation. *Engrg. Anal. Boundary Element* **26** (2002) 559–569.

6. S. Christiansen, On two methods for elimination of non-unique solutions of an integral equation with logarithmic kernel. *Appl. Anal.* **13** (1982) 1–18.
7. S. Christiansen, Modifications of some first kind integral equations with logarithmic kernel to improve numerical conditioning. *Computing* **34** (1985) 221–242.
8. S. Christiansen, The conditioning of some numerical methods for first kind boundary integral equations. *J. Comput. Appl. Math.* **67** (1996) 43–58.
9. S. Christiansen, Derivation and analytical investigation of three direct boundary integral equations for the fundamental biharmonic problem. *J. Comput. Appl. Math.* **91** (1998) 231–247.
10. S. Christiansen, Detecting non-uniqueness of solutions to biharmonic integral equations through SVD. *J. Comput. Appl. Math.* **134** (2001) 23–35.
11. C. Constanda, On non-unique solutions of weakly singular integral equations in plane elasticity. *Quart. J. Mech. Appl. Math.* **47** (1994) 261–268.
12. C. Constanda, The boundary integral equation method in plane elasticity. *Proc. Amer. Math. Soc.* **123**(11) (1995) 3385–3396.
13. C. Constanda, Integral equations of the first kind in plane elasticity. *Quart. Appl. Math.* **53**(4) (1995) 783–793.
14. M. Costabel, Boundary integral operators on Lipschitz domains: Elementary results. *SIAM J. Math. Anal.* **19**(3) (1988) 613–626.
15. M. Costabel and M. Dauge, Invertibility of the biharmonic single layer potential operator. *Integral Equations Oper. Theory* **24** (1996) 46–67.
16. R. Dautray and J.L. Lions, *Physical Origins and Classical Methods*, Mathematical Analysis and Numercial Methods for Science and Technology, Vol. 1. Springer, Berlin (2000).
17. M. Gurtin, The linear theory of elasticity. In: S. Flügge (ed.): *Encyclopedia of Physics*. Springer, Berlin (1972) pp. 1–295.
18. F. Hartmann, The physical nature of elastic layers. *J. Elasticity* **12**(1) (1982) 19–29.
19. W. He, H. Ding and H. Hu, A necessary and sufficient boundary integral formulation for plane elasticity problems. *Comm. Numer. Methods Engrg.* **12** (1996) 413–424.
20. U. Heise, The spectra of some integral operators for plane elastostatical boundary value problems. *J. Elasticity* **8**(1) (1978) 47–79.
21. U. Heise, Dependence of the round-off error in the solution of boundary integral equations on geometrical scale factor. *Comput. Methods Appl. Mech. Engrg.* **62** (1987) 115–126.
22. G. Hsiao and W. Wendland, On a boundary integral method for some exterior problems in elasticity. In: *Proc. Tbiliss. Univ. Math. Mech. Astron.* (1985) pp. 31–60.
23. M.A. Jaswon and G.T. Symm, *Integral Equation Methods in Potential Theory and Elastostatics*. Academic Press, London (1977).
24. G. Kuhn, G. Löbel and I. Potrč, Kritishes Lösungsverhalten der direkten Randelementmethode bei logarithmischen Kern. *Z. Appl. Math. Mech.* **67** (1987) 361–363.
25. W. McLean, *Strongly Elliptic Systems and Boundary Integral Equations*. Cambridge Univ. Press, Cambridge (2000).
26. C. Müller and U. Heise, Numerical calculations of eigenvalues of integral operators for plane elastostatic boundary value problems. *Comput. Methods Appl. Mech. Engrg.* **21** (1980) 17–47.
27. N.I. Muskhelishvili, *Some Basic Problems of the Mathematical Theory of Elasticity*. Soviet Union Academy of Sciences Press, Moscow (1954) (in Russian).
28. O. Steinbach and W.L. Wendland, On C. Neumann's method for second-order elliptic systems in domains with non-smooth boundaries. *J. Math. Anal. Appl.* **262** (2001) 733–748.
29. R. Vodička, V. Mantič and F. París, On the removal of non-uniqueness in the solution of elastostatic problems by Symmetric Galerkin BEM. *Internat. J. Numer. Methods Engrg.* (submitted).
30. Y. Yan and I.H. Sloan, Integral equations of the first kind with logarithmic kernels. *J. Integral Equations Appl.* **1**(4) (1988) 549–579.